Messing, J. (1983) *Methods Enzymol. 101*, 20-78.
Morley, B. J., & Campbell, R. D. (1984) *EMBO J. 3*, 153-157.
Nakamura, Y., Julier, C., Wolff, R., Holm, T., O'Connell, P., Leppert, M., & White, R. (1987) *Nucleic Acids Res. 15*, 2537-2547.
Perkins, S. J., Villiers, C. L., Arlaud, G. J., Boyd, J., Burton, D. R., Colomb, M. G., & Dwek, R. A. (1984) *J. Mol. Biol. 179*, 547-557.
Pfarr, D. S., Rieser, L. A., Woychik, R. P., Rottman, F. M., Rosenberg, M., & Reff, M. E. (1986) *DNA 5*, 115-122.
Reid, K. B. M., & Porter, R. R. (1981) *Annu. Rev. Biochem. 50*, 433-464.
Reid, K. B. M., Bentley, D. R., Campbell, R. D., Chung, L. P., Sim, R. B., Kristensen, T., & Tack, B. F. (1986) *Immunol. Today 7*, 230-234.
Sanger, F., Nicklen, S., & Coulson, A. R. (1977) *Proc. Natl. Acad. Sci. U.S.A. 74*, 5463-5467.
Schumaker, V. N., Hanson, D. C., Kilchherr, E., Phillips, M. L., & Poon, P. H. (1986) *Mol. Immunol. 23*, 557-565.
Schumaker, V. N., Zavodszky, P., & Poon, P. H. (1987) *Annu. Rev. Immunol. 5*, 21-42.
Sim, R. B., Porter, R. R., Reid, K. B. M., & Gigli, I. (1977) *Biochem. J. 163*, 219-227.
Spycher, S. E., Nick, H., & Rickli, E. E. (1986) *Eur. J. Biochem. 156*, 49-57.
Stanley, K. K., Page, M., Campbell, A. K., & Luzio, J. P. (1986) *Mol. Immunol. 23*, 451-458.
Stenflo, J., Lundwall, A., & Dahlbäck, B. (1987) *Proc. Natl. Acad. Sci. U.S.A. 84*, 368-372.
Südhof, T. C., Goldstein, J. L., Brown, M. S., & Russell, D. W. (1985) *Science (Washington, D.C.) 228*, 815-822.
Tosi, M., Young, R. A., Hagenbüchle, O., & Schibler, U. (1981) *Nucleic Acids Res. 9*, 2313-2323.
Tosi, M., Journet, A., Colomb, M., & Meo, T. (1985) *Complement 2*, 79.
Tosi, M., Duponchel, C., Bourgarel, P., Colomb, M., & Meo, T. (1986a) *Gene 42*, 265-272.
Tosi, M., Journet, A., Lyonnet, D., Colomb, M., & Meo, T. (1986b) *Protides Biol. Fluids 34*, 453-456.
Villiers, C. L., Arlaud, G. J., & Colomb, M. G. (1985) *Proc. Natl. Acad. Sci. U.S.A. 82*, 4477-4481.
Weiss, V., Fauser, C., & Engel, J. (1986) *J. Mol. Biol. 189*, 573-581.
Wharton, K. A., Johansen, K. M., Xu, T., & Artavanis-Tsakonas, S. (1985) *Cell (Cambridge, Mass.) 43*, 567-581.
Von Heijne, G. (1986) *Nucleic Acids Res. 14*, 4683-4690.
Ziccardi, R. J. (1986) *J. Immunol. 136*, 3378-3383.

Investigation of Transition-State Stabilization by Residues Histidine-45 and Threonine-40 in the Tyrosyl-tRNA Synthetase†

Robin J. Leatherbarrow* and Alan R. Fersht*

Department of Chemistry, Imperial College of Science and Technology, London SW7 2AY, U.K.

Received May 14, 1987; Revised Manuscript Received August 13, 1987

ABSTRACT: We have analyzed various mutations involving residues Thr-40 and His-45 in the tyrosyl-tRNA synthetase of *Bacillus stearothermophilus*. The utilization of binding energy in catalysis of tyrosyl adenylate formation from tyrosine and ATP was determined from the free energy profiles for the mutant enzymes. Our results confirm that the side chains of Thr-40 and His-45 provide a binding site for the pyrophosphoryl portion of the transition state of this reaction and for pyrophosphate in the reverse reaction. Deletion of these side chains destabilizes the transition-state by 4.9 and 4.1 kcal mol^{-1}, respectively, consistent with a charged hydrogen-bonding interaction. To examine the role of His-45 further, we constructed the potentially conservative mutations His → Gln-45 and His → Asn-45. Both mutant enzymes are debilitated compared with the native enzyme. The His → Gln-45 enzyme is more active than enzyme in which the complete side chain is deleted (His → Ala-45), and so in this location glutamine is a semiconservative replacement. In contrast, the His → Asn-45 mutation is significantly worse than simple deletion of the side chain, indicating that asparagine at this position causes active destabilization of the transition state compared to His → Ala-45. The amide $-NH_2$ of glutamine may be considered stereochemically equivalent to the ϵ-NH of histidine whereas the amide $-NH_2$ of asparagine is comparable to the δ-NH of histidine. The results suggest that the ϵ-NH rather than the δ-NH group of His-45 is involved in the transition-state stabilization. The large range of effects from "conservative" substitutions at position 45 illustrates the danger of inferring information about binding energies when alternative interactions are introduced by mutation.

The tyrosyl-tRNA synthetase of *Bacillus stearothermophilus* has been the subject of extensive studies using protein engineering [see Leatherbarrow and Fersht (1986) for a recent review]. The experiments have involved systematic mutation of residues around the active site of the enzyme in a manner designed to remove interactions with substrates, products, intermediates, and transition states. Comparison of native and mutant enzymes has allowed us to determine the apparent contribution of various side chains to binding and catalysis (Fersht et al., 1985, 1986a,b).

Tyrosyl-tRNA synthetase catalyzes the formation of enzyme-bound tyrosyl adenylate (Tyr-AMP) from tyrosine (Tyr)

† This work was funded by the MRC of the U.K.

0006-2960/87/0426-8524$01.50/0

and ATP as the first step in the synthesis of aminoacyl-tRNA (eq 1). Catalysis is achieved by preferential binding of the

$$E + ATP + Tyr \rightleftharpoons E{\cdot}Tyr\text{-}AMP + PP_i \quad (1)$$

transition state. Model building of the putative transition-state complex implicated a role for the side chains of His-45 and Thr-40; this was verified by protein engineering to create His → Gly-45 and Thr → Ala-40 mutant enzymes in which these interactions were removed (Leatherbarrow et al., 1985). The role of His-45 is particularly interesting since it forms part of a small region (consensus sequence -His_{45}-Ile-Gly-His-) that is conserved among several aminoacyl-tRNA synthetase enzymes (Webster et al., 1984; Jones et al., 1986; Borgford et al., 1987).

In this paper we present the complete free energy profiles for these mutants at positions 40 and 45 together with full characterization of four further mutations at these positions. The results confirm the role of Thr-40 and His-45 in transition-state stabilization and give some indication of the importance of conserving a histidine at position 45. They also illustrate some of the problems associated with explaining the properties of semiconservative substitutions, where the effects of both removing and introducing interactions need to be considered.

Materials and Methods

Construction of Mutant Enzymes. The mutant enzymes His → Gly-45 and Thr → Ala-40 have been described earlier (Leatherbarrow et al., 1985). The other mutant tyrosyl-tRNA synthetases were constructed by coupled priming and amber selection (Carter et al., 1985). The following oligonucleotides, which were synthesized with an Applied Biosystems 380B DNA synthesizer, were used for the mutagenesis experiments: His → Ala-45, 5′-GGCCGATAG*C*AAACTGT-3′; His → Gln-45, 5′-GTGGCCGATC*TGCAAAC-3′; Thr → Gly-40, 5′-CTGTCCGGCC*C*C*CGGGTCAA-3′. Mismatched bases are indicated by a following asterisk. The sequences of mutant genes were confirmed by dideoxy sequencing (Sanger et al., 1977). The mutant His → Asn-45 was a gift from Dr. Greg Winter.

Mutant protein was isolated as described for other tyrosyl-tRNA synthetase mutants (Lowe et al., 1985) by ion-exchange chromatography on DEAE-Sephacel followed by fast protein liquid chromatography (FPLC) with mono-Q ion-exchange resin (Pharmacia). All enzymes were chromatographically homogeneous on sodium dodecyl sulfate–polyacrylamide gel electrophoresis (Na_2DodSO_4–PAGE).

Kinetic Measurements. Unless indicated otherwise, all experiments were performed at 25 °C and pH 7.78 in a standard buffer of 0.144 tris(hydroxymethyl)aminomethane hydrochloride (Tris-HCl), 0.1 mM phenylmethanesulfonyl fluoride (PMSF), 14 mM 2-mercaptoethanol, and 10 mM Mg^{2+}.

All the enzymes studied catalyze the formation of tyrosyl adenylate from tyrosine and ATP at a much lower rate than does the native enzyme. For enzymes with k_{-3} greater than $\sim 0.1\ s^{-1}$, the formation of tyrosyl adenylate was followed by stopped-flow fluorescence (Fersht et al., 1975; Wells & Fersht, 1986). For enzymes with k_{-3} less than this, formation of enzyme-bound tyrosyl adenylate from [^{14}C]tyrosine and ATP was monitored by filtration through nitrocellulose filters (Sartorius). A solution (280 μL) of standard buffer containing ATP (0.25–20 mM), [^{14}C]Tyr (30 μM), and inorganic pyrophosphatase (0.001 unit mL^{-1}) was incubated at 25 °C, and prewarmed enzyme (20 μL of ~10 μM) was added to initiate the reaction. Twelve aliquots of 20 μL were periodically taken over at least four half-lives of the reaction, filtered through nitrocellulose filters, washed with 5 mL of ice-cold standard buffer, and dried, and the retained E·[^{14}C]Tyr-AMP was assayed by liquid scintillation counting. Rate constants were calculated by nonlinear regression to a first-order theoretical curve (Leatherbarrow, 1987). The observed rate constant for formation of E·Tyr-AMP (k_{obsd}) was corrected where necessary for the loss of Tyr-AMP by dissociation or hydrolysis. [$k_{obsd} = k + k_{dec}$, where k is the rate constant for formation and k_{dec} is the rate constant for loss of Tyr-AMP. The steady-state level of E·Tyr-AMP formed is given by $[E_0]k/(k + k_{dec})$.] The kinetic constants k_3 and K'_a were calculated from the variation of k with [ATP].

Scheme I

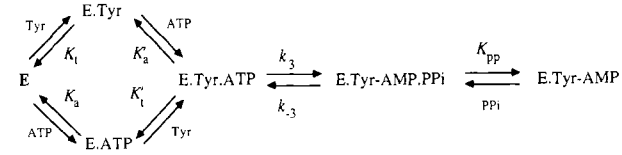

The rate of pyrophosphorylysis was measured in a similar manner. Enzyme-bound [^{14}C]tyrosyl adenylate was prepared by incubating enzyme (0.5 mL, 2 μM) with [^{14}C]tyrosine (10 μM) and Mg-ATP (5 mM) for 40 min at 25 °C followed by gel filtration through Sephadex G-50 (medium, 1 × 15 cm) at 4 °C into standard buffer. For all the enzymes studied, the isolated adenylate was stable at 4 °C for several hours. Pyrophosphate (up to 16 mM) was added to a solution of the E·[^{14}C]Tyr-AMP complex in standard buffer (with additional Mg^{2+} equivalent to the added pyrophosphate) to initiate the reaction. Five aliquots of 20 μL were periodically taken over two to three half-lives of the reaction, filtered through nitrocellulose filters, washed with 5 mL of ice-cold standard buffer, and dried, and the retained E·[^{14}C]Tyr-AMP was assayed by scintillation counting. None of the enzymes studied displayed saturation kinetics for the rate of pyrophosphorylysis versus [pyrophosphate] under the conditions used (higher concentrations are not possible due to the limited solubility of magnesium pyrophosphate). Under these conditions the plot of rate of decay of E·[^{14}C]Tyr-AMP versus [pyrophosphate] is linear with a slope of k_{-3}/K_{pp}, which was calculated by linear regression.

Binding of Tyrosine. The binding constant of tyrosine to the unligated enzyme was determined by equilibrium dialysis with [^{14}C]tyrosine (2–100 μM) (Fersht et al., 1975). All of the enzymes studied bound 1 mol of tyrosine/mol of enzyme.

Results

Calculation of the complete free energy profile for the reactions catalyzed by tyrosyl-tRNA synthetase (Scheme I) requires measurement of (i) the dissociation constant for tyrosine, K_t, from the enzyme–tyrosine complex (E·Tyr), (ii) the dissociation constant of ATP from enzyme–tyrosine–ATP complex (E·Tyr·ATP), K'_a, (iii) the forward rate constant for the formation of tyrosyl adenylate, k_3, (iv) the rate constant for pyrophosphorolysis of the enzyme–tyrosyl adenylate complex (E·Tyr-AMP), k_{-3}, and (v) the dissociation constant of pyrophosphate from the enzyme-tyrosyl adenylate–PP_i complex (E·Tyr-AMP·PP_i), K_{pp} (Wells & Fersht, 1986). The values of these rate and equilibrium constants for the wild-type tRNA synthetase and for the mutants Thr → Ala-40, Thr → Gly-40, His → Gly-45, His → Ala-45, His → Gln-45, and His → Asn-45 are given in Table I. All these mutations result in a large increase in K_{pp} ($K_{pp} > 10$ mM). Since the solubility of magnesium pyrophosphate at pH 7.78 is approximately 4 mM, saturation kinetics are not observed for pyro-

Table I: Rate and Dissociation Constants for the Formation of Enzyme-Bound Tyrosyl Adenylate[a]

enzyme	K_t (μM)	K'_A (mM)	k_3 (s^{-1})	k_{-3}/K_{pp} (M^{-1} s^{-1})
His → Gly-45	43	1.3	0.16 (f)	307
His → Ala-45	31	5.0	0.10 (s)	43
His → Gln-45	14	6.1	0.80 (f)	314
His → Asn-45	23	1.6	0.0032 (s)	3.3
Thr → Ala-40	11	3.8	0.0055 (s)	3.6
Thr → Gly-40	12	3.7	0.009 (s)	3.2
wild type[b]	12	4.7	38	27 200

[a] Experiments were performed at 25 °C and pH 7.78 (144 mM Tris-HCl, 10 mM $MgCl_2$, 14 mM 2-mercaptoethanol, and 1 unit/mL pyrophosphate). Values of K'_A, the dissociation constant of ATP from the E·Tyr-ATP complex, and k_{-3}, the forward rate constant for the formation of tyrosyl adenylate, were determined by stopped-flow fluorescence for the faster enzymes (f) and manual filter assays for the slower ones (s). Values of k_{-3} (see Scheme I) are extrapolated to saturating levels of ATP and tyrosine. K_t, the dissociation constant of tyrosine from the E·Tyr complex, was determined by equilibrium dialysis. k_{-3}/K_{pp} is calculated from the slope of the plot of rate of hydrolysis of E·Tyr-AMP versus [PP_i]. [b] From Wells and Fersht (1986).

Table II: Gibbs Free Energies of Complexes of Wild-Type and Mutant Enzymes[a]

enzyme	$G_{E\cdot Tyr}$	$G_{E\cdot Tyr\cdot ATP}$	$G_{[E\cdot Tyr\cdot ATP]^*}$	$G_{E\cdot Tyr\cdot AMP}$
His → Gly-45	−5.95	−9.89	8.64	−5.41
	(0.76)	(0.00)	(3.23)	(0.58)
His → Ala-45	−6.15	−9.28	9.52	−5.70
	(0.56)	(0.61)	(4.11)	(0.29)
His → Gln-45	−6.62	−9.64	7.94	−6.10
	(0.09)	(0.25)	(2.53)	(−0.11)
His → Asn-45	−6.32	−10.14	10.71	−6.02
	(0.39)	(−0.25)	(5.30)	(−0.03)
Thr → Ala-40	−6.76	−10.06	10.46	−6.22
	(−0.05)	(−0.17)	(5.05)	(−0.23)
Thr → Gly-40	−6.71	−10.02	10.21	−6.55
	(0.00)	(−0.13)	(4.80)	(−0.23)
wild type[b]	−6.71	−9.89	5.41	−5.99

[a] Standard state = 1 M tyrosine, 1 M ATP, 1 M PP_i, and free enzyme (G_E = 0). The numbers in parentheses show the difference in free energy between the mutant and wild-type enzymes for each complex. [b] From Wells and Fersht (1986).

phosphorolysis of E·Tyr-AMP in the mutants studied. The ratio of k_{-3}/K_{pp} can be determined, however, from the gradient of the rate of reaction versus [PP_i] plot for pyrophosphorolysis.

The effect of these mutations on the free energy profile of the reaction is given in Table II and also shown in the form of difference free energy plots (Figure 1). Such plots record the effect of the mutations on the various enzyme-bound complexes by plotting $\Delta G_{wild\text{-}type} - \Delta G_{mutant}$, where ΔG is the difference in free energy between the ligated and unligated enzyme, calculated from standard thermodynamic equations (Wells & Fersht, 1986). It is not possible to calculate the free energy level of the E·Tyr-AMP·PP_i complex for these mutant enzymes in the absence of a value for K_{pp}. However, a *minimum* value for the difference can be estimated assuming K_{pp} > 10 mM, and this is indicated.

For all the mutations studied the major effect for the forward reaction is on the rate rather than on the substrate dissociation constants. The binding of pyrophosphate is greatly altered while the tyrosyl adenylate free energy level is unaffected. The net result is a characteristic difference free energy profile with the largest effects being on the states [E·Tyr·ATP]* and E·Tyr-AMP·PP_i.

Discussion

The side chains of Thr-40 and His-45 are positioned far from tyrosyl adenylate in the X-ray structure of the E·Tyr-AMP complex (Brick & Blow, 1987). However, model

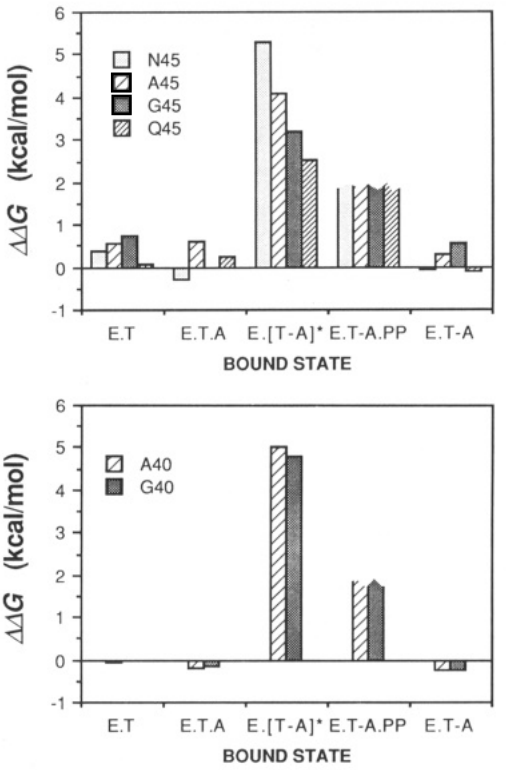

FIGURE 1: Difference free energy profiles (Gibbs free energy levels of complexes of mutant enzymes minus those for wild type). The mutants are as follows: N45, His → Asn-45; A45, His → Ala-45; G45, His → Gly-45; Q45, His → Gln-45; A40, Thr → Ala-40; G40, Thr → Gly-40. Free energies are measured in kcal mol^{-1} with standard states of 1 M tyrosine, 1 M ATP, and 1 M PP_i. The enzyme-bound states are as follows: T = tyrosine; A = ATP; [T-A]* = transition state; T-A = tyrosyl adenylate; PP = pyrophosphate. The jagged top to the difference energies of the E·T-A·PP complex represents a minimum value since the dissociation constants of PP_i are immeasurably high.

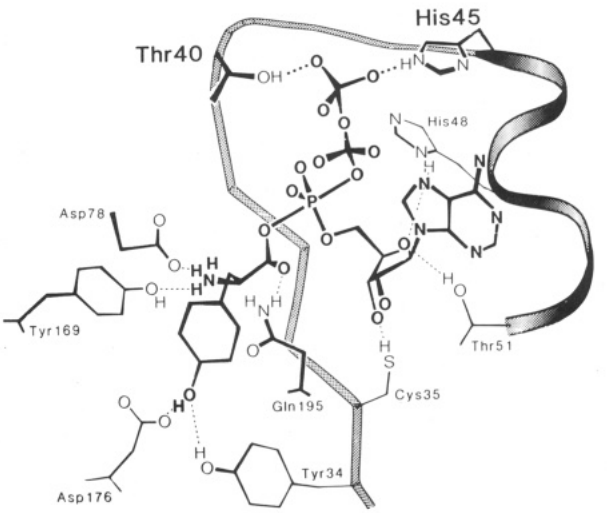

FIGURE 2: Model of the transition-state complex showing how interactions may be made from the side chains of Thr-40 and His-45 to the γ-phosphate of the transition state [from Leatherbarrow et al. (1985)].

building has shown that it is possible for them to interact with the transition state via the γ-phosphate group (Figure 2). Our results show that total removal of these side chains (Thr → Ala-40, Thr → Gly-40, His → Ala-45, His → Gly-45) results in a large destabilization of the transition state and E·Tyr-AMP·PP_i complexes. The latter is caused by effects on pyrophosphate binding and not on alteration of the energy level

of E·Tyr-AMP. Thr-40 and His-45 therefore form part of the binding site for pyrophosphate in the reverse reaction, and for the pyrophosphoryl portion of the transition state.

Mutation of Side Chains to Glycine and Alanine. The simplest strategy for examining the function of a side chain is the mutation of an interacting residue to an amino acid with a short side chain. Glycine and alanine are the amino acids with the shortest side chains. Glycine is the shorter of the two since it lacks the β-carbon, and so mutation to glycine introduces much greater potential for flexibility.

(A) Thr → Gly-40 and Thr → Ala-40. Mutation at position 40 to replace threonine by alanine results in a very large effect on the stability of the transition state, which is destabilized by 5.05 kcal mol^{-1} compared with the native enzyme. Unless the mutation has caused a gross structural perturbation in the enzyme, this effect can be considered to result from either (i) the loss of an interaction worth 5.05 kcal mol^{-1} (relative to the mutant) or (ii) an active destabilization of the transition state, accompanied by some loss of some binding energy. Our previous model-building studies indicated that it is likely that an interaction would be lost on mutation of Thr-40 (Leatherbarrow et al., 1985). However, mutation to Ala will place a hydrophobic methyl group adjacent to the charged transition state; this could destabilize this state relative to free solution by preventing maximal solvation. To examine this possibility, we constructed the mutant Thr → Gly-40. If the Thr → Gly-40 mutation produced less transition-state destabilization, then this would indicate some active destabilization by the β-methyl of Ala-40. However, the kinetic properties of Thr → Gly-40 are similar to those of Thr → Ala-40. This suggests that the intrinsic stabilization of the transition state by Thr-40 is indeed ~5 kcal mol^{-1} relative to a mutant, although it is possible that the –H side chain of glycine is also providing active destabilization in a similar manner.

(B) His → Gly-45 and His → Ala-45. The free energy profiles of these two mutant enzymes are similar but not identical, differing by 0.88 kcal mol^{-1} in the free energy of the transition-state complex. Both show some perturbation to the binding of tyrosine to the free enzyme. This is more pronounced in the His → Gly-45 enzyme (0.76 kcal mol^{-1}) than in the His → Ala-45 enzyme (0.56 kcal mol^{-1}). This effect only occurs for tyrosine binding in the absence of ATP (measured by equilibrium dialysis); when tyrosine binding in studied in the presence of ATP by a kinetic method, the binding constant is unaffected (Leatherbarrow et al., 1985). It is possible that this effect on tyrosine binding reflects some conformational alterations in these mutant enzymes. Alternatively, it could be due to the removal of long-range electrostatic interactions between the charged histidine residue and the tyrosine carboxyl group.

(C) Replacement of His-45 by Gln or Asn. His-45 of the tyrosyl-tRNA synthetase is the first histidine of the consensus sequence "HIGH" found in many aminoacyl-tRNA synthetases. The importance of this residue is illustrated by the large effect on the rate of reaction when this His is replaced by Gly or Ala. It is of interest, however, to examine what happens in the event of a conservative replacement. The second His in the HIGH consensus sequence is replaced by Asn in the highly homologous tyrosyl-tRNA synthetase from *Bacillus caldotenax* (Jones et al., 1986), consistent with the most conservative replacements for histidine being Asn and Gln. These structures may be superimposed on an imidazole ring (Figure 3). To a simple approximation the amide groups of Asn and Gln can be considered to occupy analogous positions to the δ- and ε-NH groups of the imidazole. For His-48,

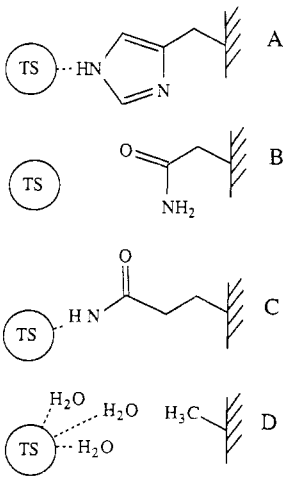

FIGURE 3: Possible effects of mutations at position 45 on interactions with the transition state (TS). Also illustrated is the approximate equivalence in position of the nitrogen atoms of asparagine and glutamine with the corresponding nitrogen atoms of the histidine imidazole ring. (A) His-45. Interactions are made between the ε-N of the imidazole and the transition state, which result in stabilization of this state. (B) Asn-45. No interactions are possible to the transition state. In addition, the bulk of the side chain restricts solvation of the transition state, resulting in a large deleterious effect. (C) Gln-45. Some interaction between the $-NH_2$ group and the transition state is possible (although the experiments show that these are less optimal than interactions to His-45). (D) Ala-45. An interaction with the transition state has been lost compared with the wild-type enzyme. However, the small side chain allows the transition state to be solvated. This results in a destabilization of the transition state which is intermediate to that shown by the His → Asn-45 and the His → Gln-45 mutant enzymes.

previous studies have indicated that mutagenesis to Asn is almost completely conservative in nature, whereas His → Gln-48 shows marked deterioration in its kinetic properties (Lowe et al., 1985). This is consistent with an interaction involving the δ-NH group of His-48, which can be substituted by interactions to the δ-NH_2 of Asn-48. The kinetic properties of His → Asn-45 and His → Gln-45 are given in Table I. In contrast with mutations at position 48, neither of these mutant enzymes has properties that are similar to those of the native enzyme. The difference free energy profiles for all the 45-position mutants show the same overall shape, indicating that in all cases the same interactions have been perturbed.

The magnitude of the effect on the transition-state from energy level varies markedly between the various position 45 mutant enzymes. It is instructive to consider His → Ala-45 as a reference point, since in this mutation the imidazole side chain has been completely removed, leaving just the β-carbon. The value of $\Delta\Delta G_{[E\cdot T\cdot A]^*}$ for Ala-45 gives some indication, therefore, of the effective strength of the original interaction between His-45 and the transition state. With a value of 4.11 kcal mol^{-1}, this is consistent with the loss of a charged hydrogen-bonding interaction (Fersht et al., 1985). Mutation that involves *replacement* of a side chain will have an effect equal to the sum of interactions lost to the original side chain and the interactions gained to the new side chain. The difference between $\Delta\Delta G_{[E\cdot T\cdot A]^*}$ for Ala-45 and $\Delta\Delta G_{[E\cdot T\cdot A]^*}$ for Asn-45 or Gln-45 will therefore be equal to the free energy of interaction with the new side chain alone. On this basis, the interactions between the transition state and His-45, Gln-45, and Asn-45 are worth 4.1, 1.6, and –1.2 kcal mol^{-1}, respectively, relative to the His → Ala-45 mutant enzyme. The difference between His → Gln-45 and His → Asn-45 is striking and significant in that they have opposite effects: Gln offers marked improvement over Ala; Asn, a marked deteri-

oration. Gln-45 is therefore a partially conservative replacement for His-45, although the interaction with the glutamine side chain contributes only around 40% of the binding energy provided by the histidine. This could be for two reasons: (i) the original histidine is charged, and the glutamine cannot replace the charge; (ii) the interaction with the glutamine is not optimized sterically. Using the analogy between the structures of histidine, glutamine, and asparagine (Figure 3), these results provide evidence that the original interaction is between the transition state and the ϵ-NH of His-45. This is in agreement with our previous model-building studies (Leatherbarrow et al., 1985).

Transition-State Destabilization. The mutation His → Asn-45 results in a destabilization of the transition state by 1.2 kcal mol^{-1} over and above the 4.1 kcal mol^{-1} lost on removing the side chain by the mutation His → Ala-45. The probable explanation for this involves solvation of the transition state, which is shown schematically in Figure 3. In the native enzyme the transition state is stabilized by an interaction with the ϵ-NH of the imidazole. In Gln-45 this can be replaced by an analogous interaction with the amide group. The experimental results indicate that although some interaction is made, it is weaker than the original. In Ala-45 the hydrogen bond is removed, but this would allow the transition state to be solvated as water would occupy the vacated space. Mutation to Asn-45, as well as removing the original hydrogen bond, will result in partial occlusion of the site and so interfere with the solvation. The mutation His → Asn-45 therefore exacts a double penalty, resulting in the extremely large effect on the rate of reaction.

The similarity between the energetic effects of the mutations His → Asn-45 and Thr → Ala-40 makes it tempting to speculate that in both cases there is a similar active destabilization of the transition state. However, the mutant enzyme Thr → Gly-40 has similar energetic properties to the Thr → Ala-40 enzyme, indicating either minimal destabilization in this case or equivalent destabilization in each of the position-40 mutations.

Effect of Side-Chain Replacement. In a site-directed mutagenesis experiment, removal of a side chain that interacts with enzyme-bound reagents will result in destabilization of this state. Judicious replacement of side chains that form hydrogen bonds for ones that lack appropriate acceptor/donor groups allows estimation of the apparent strength of the original interaction. Of the mutations described here, all the →Gly and →Ala changes fall into this category of "side-chain deletions" (Fersht et al., 1987). In general, however, replacement of one side chain for another will, as well as deleting the original interaction, introduce a different interaction. The mutations His → Asn-45 and His → Gln-45 are examples of such "semiconservative replacements". As is illustrated here, the properties of these mutations are more complex. In particular, the difference free energy for such mutants is *not* a measure of the hydrogen-bond strength involving the original side chain. This consideration is important when interpreting the results of mutagenesis. For example, the mutation His → Gln-45 in dihydrofolate reductase from *Escherichia coli* is found to result in only a small reduction in binding energy, which was considered to be inconsistent with the loss of a charged hydrogen bond (Chen et al., 1985). Clearly, this mutation is likely to be analogous to the His → Gln-45 mutation described above, with the loss of the original interactions being compensated to some extent by the gain of an interaction to the glutamine side chain; it would be interesting to know the effect of an His → Ala-45 mutation in dihydrofolate reductase.

Conservation of Residues 40 and 45. Residue His-45 is conserved in five different aminoacyl-tRNA synthetases (Borgford et al., 1987), implying a similar role of transition-state stabilization in all these enzymes. Indeed, the mutation His → Asn at this position in the valyl-tRNA synthetase has been shown to result in similar effects as the corresponding mutation in the tyrosyl-tRNA synthetase (Borgford et al., 1987). Conservation of Thr-40 is not so pronounced, although the mutation Thr → Ala at this position in valyl-tRNA synthetase again has a similar effect to the corresponding mutation in the tyrosyl enzyme (Borgford et al., 1987).

It seems likely that those aminoacyl-tRNA synthetase enzymes that possess the HIGH consensus sequences do so in order to conserve a common mechanism of aminoacylation. Although the second histidine of this sequence may be substituted by asparagine, the side chain of the first histidine, His-45, seems essential if the reaction is to proceed at the wild-type rate.

References

Borgford, T. J., Gray, T. E., Brand, N. J., & Fersht, A. R. (1987) *Biochemistry 26*, 7246–7250.

Brick, P., & Blow, D. M. (1987) *J. Mol. Biol. 194*, 287–297.

Carter, P., Bedouelle, H., & Winter, G. (1985) *Nucleic Acids Res. 13*, 4431–4443.

Chen, J.-T., Mayer, R. J., Fierke, C. A., & Benkovic, S. J. (1985) *J. Cell. Biochem. 29*, 17–26.

Fersht, A. R., Mulvey, R. S., & Koch, G. L. E. (1975) *Biochemistry 14*, 13–18.

Fersht, A. R., Shi, J.-P., Knill-Jones, J., Lowe, D. M., Wilkinson, A. J., Blow, D. M., Brick, P., Carter, P., Waye, M. M. Y., & Winter, G. (1985) *Nature (London) 314*, 235–238.

Fersht, A. R., Leatherbarrow, R. J., & Wells, T. N. C. (1986a) *Philos. Trans. R. Soc. London, A 317*, 305–320.

Fersht, A. R., Leatherbarrow, R. J., & Wells, T. N. C. (1986b) *Nature (London) 322*, 284–286.

Fersht, A. R., Leatherbarrow, R. J., & Wells, T. N. C. (1987) *Biochemistry 26*, 6030–6038.

Jones, M. D., Lowe, D. M., Borgford, T., & Fersht, A. R. (1986) *Biochemistry 25*, 1887–1891.

Leatherbarrow, R. J. (1987) *Enzfitter. A Non-Linear Regression Data Analysis Program for the IBM PC*, Elsevier Science, Amsterdam.

Leatherbarrow, R. J., & Fersht, A. R. (1986) *Protein Eng. 1*, 7–16.

Leatherbarrow, R. J., Winter, G., & Fersht, A. R. (1985) *Proc. Natl. Acad. Sci. U.S.A. 82*, 7840–7844.

Lowe, D. M., Fersht, A. R., Wilkinson, A. J., Carter, P., & Winter, G. (1985) *Biochemistry 24*, 5106–5109.

Sanger, F., Nicklen, S., & Coulson, A. R. (1977) *Proc. Natl. Acad. Sci. U.S.A. 74*, 5463–5467.

Webster, T., Tsai, H., Kula, M., Mackie, G. A., & Schimmel, P. (1984) *Science (Washington, D.C.) 226*, 1315–1317.

Wells, T. N. C., & Fersht, A. R. (1986) *Biochemistry 25*, 1181–1186.